Strong-field double ionization of rare gases

J. L. Chaloupka, R. Lafon, L. F. DiMauro
Chemistry Department, Brookhaven National Laboratory, Upton, NY 11973 USA
jcha@bnl.gov

P. Agostini
SPAM, Centre d'Etudes de Saclay, 91191 Gif Sur Yvette, France

K. C. Kulander
TAMP, Lawrence Livermore National Laboratory, Livermore, CA 94551 USA

Abstract: We have studied the double ionization of helium and other rare gases using an electron-ion coincidence technique. With this scheme, the electron energy spectrum correlated to the creation of a doubly charged ion may be compiled. In all cases, the observed double ionization electron distributions are similar and enhanced at high energies, while the single ionization spectra exhibit distinct differences.

OCIS codes: (020.4180) Multiphoton processes; (270.6620) Strong-field processes

References and links

1. P. B. Corkum, "Plasma perspective on strong field multiphoton ionization," Phys. Rev. Lett. **71**, 1994-1997 (1993).
2. J. B. Watson, A. Sanpera, D. G. Lappas, P. L. Knight, and K. Burnett, "Nonsequential double ionization of helium," Phys. Rev. Lett. **78**, 1884-1887 (1997).
3. J. S. Parker, E. S. Smyth, and K. T. Taylor, "Intense-field multiphoton ionization of helium," J. Phys. B **31**, L571-L578 (1998).
4. M. A. Kornberg and P. Lambropoulos, "Photoelectron energy spectrum in 'direct' two-photon double ionization of helium," J. Phys. B **32**, L603-L613 (1999).
5. A. Becker and F. H. M. Faisal, "Interpretation of momentum distribution of recoil ions from laser induced nonsequential double ionization," Phys. Rev. Lett. **84**, 3546-3549 (2000).
6. R. Panfili, C. Szymanowski, W.-C. Liu, and J. H. Eberly, "Spectroscopy in the neighborhood of the double ionization knee" in *Multiphoton Processes*, L.F. DiMauro, R.R. Freeman, K.C. Kulander, eds., (American Institute of Physics, New York, NY 2000).
7. M. Lein, E. K. U. Gross, and V. Engel, "Intense-field double ionization of helium: identifying the mechanism," Phys. Rev. Lett. **85**, 4707-4710 (2000).
8. G. L. Yudin and M. Ivanov, "Physics of correlated double ionization of atoms in intense laser fields: quasistatic tunneling limit," Phys. Rev. A, in press (2001).
9. Th. Weber, H. Giessen, M. Weckenbrock, G. Urbasch, A. Staudte, L. Spielberger, O. Jagutzki, V. Mergel, M. Vollmer, and R. Dörner, "Correlated electron emission in multiphoton double ionization," Nature **405**, 658-661 (2000).
10. R. Moshammer, B. Feuerstein, W. Schmitt, A. Dorn, C. D. Schröter, J. Ullrich, H. Rottke, C. Trump, M. Wittman, G. Korn, K. Hoffman, and W. Sandner, "Momentum distributions of Ne^{n+} ions created by an intense ultrashort laser pulse," Phys. Rev. Lett. **84**, 447-450 (2000).
11. Th. Weber, M. Weckenbrock, A. Staudte, L. Spielberger, O. Jagutzki, V. Mergel, F. Afaneh, G. Urbasch, M. Vollmer, H. Giessen, and R. Dörner, "Recoil-ion momentum distributions for single and double ionization of helium in strong laser fields," Phys. Rev. Lett. **84**, 443-446 (2000).
12. B. Witzel, N. A. Papadogiannis, and D. Charalambidis, "Charge-state resolved above threshold ionization," Phys. Rev. Lett. **85**, 2268-2271 (2000).
13. R. Lafon, J. L. Chaloupka, B. Sheehy, P. M. Paul, P. Agostini, K. C. Kulander, and L. F. DiMauro, "Electron energy spectra from intense laser double ionization of helium," Phys. Rev. Lett., in press (2001).
14. D. N. Fittinghoff, P. R. Bolton, B. Chang, and K. C. Kulander, "Observation of nonsequential double ionization of helium with optical tunneling," Phys. Rev. Lett. **69**, 2642-2645 (1992).
15. B. Walker, B. Sheehy, L. F. DiMauro, P. Agostini, K. J. Schafer, and K. C. Kulander, "Precision measurement of strong field double ionization of helium," Phys. Rev. Lett. **73**, 1227-1230 (1994).
16. S. Larochelle, A. Talebpour, and S. L. Chin, "Non-sequential multiple ionization of rare gas atoms in a Ti:Sapphire laser field," J. Phys. B **31**, 1201-1214 (1998).

#30647 - $15.00 US Received February 02, 2001; Revised March 02, 2001

17. E. Mevel, P. Breger, R. Trainham, G. Petite, P. Agostini, A. Migus, J.-P. Chambaret, and A. Antonetti, "Atoms in strong optical fields: evolution from multiphoton to tunnel ionization," Phys. Rev. Lett. **70**, 406-409 (1993).
18. U. Mohideen, M. H. Sher, H. W. K. Tom, G. D. Aumiller, O. R. Wood II, R. R. Freeman, J. Bokor, and P. H. Bucksbaum, "High intensity above-threshold ionization of He," Phys. Rev. Lett. **71**, 509-512 (1993).
19. B. Walker, B. Sheehy, K. C. Kulander, and L. F. DiMauro, "Elastic rescattering in the strong field tunneling limit," Phys. Rev. Lett. **77**, 5031-5034 (1996).
20. B. Sheehy, R. Lafon, M. Widmer, B. Walker, L. F. DiMauro, P. A. Agostini, and K.C. Kulander, "Single- and multiple-electron dynamics in the strong-field tunneling limit," Phys. Rev. A **58**, 3942-3952 (1998).
21. K. J. Schafer, B. Yang, L. F. DiMauro, and K. C. Kulander, "Above threshold ionization beyond the high harmonic cutoff," Phys. Rev. Lett. **70**, 1599-1602 (1993).
22. V. Stert, W. Radloff, C. P. Schulz, and I. V. Hertel, "Ultrafast photoelectron spectroscopy: femtosecond pump-probe coincidence detection of ammonia cluster ions and electrons," Eur. Phys. J. D **5**, 97-106 (1999).

1. Introduction

As is evidenced by this Focus Issue, the double ionization of atoms by strong fields has been the subject of a great deal of recent interest. As the power and sophistication of theoretical calculations has advanced [1-8], so too have the techniques of the experimentalist [9-13]. In the past, the singly and doubly charged ion yields have been meticulously recorded over many orders of magnitude [14-16]. The electron energy spectra from the single ionization process have also been observed [17-20]. Each of these measurements has provided insight into the physics of the interaction of an intense laser field with an atom. The yields for single ionization showed good agreement with single-active-electron models, but the double ionization yields showed a dramatic enhancement at low intensities. It was postulated that a form of electron correlation was contributing to the increased rate of double ionization. One such scheme that has gained the widest acceptance involves the rescattering of the first liberated electron with the ion core [21], resulting in an e-2e impact ionization [1].

Very recent experimental advances have led to the measurement of the doubly charged ion recoil momentum, as well as the energy of the electrons correlated with the double ionization process. Cold target recoil ion momentum spectroscopy (COLTRIMS) has been used to measure the ion momenta in argon [9], neon [10] and helium [11], as well as the electron momenta in argon [9]. Schemes utilizing electron-ion coincidence have been used to measure the electron energy spectra generated in the double ionization of xenon [12] and helium [13]. In this article, we present the single and double ionization electron energy spectra from xenon, krypton, argon, neon and helium. In this survey of the rare gases, each measurement was taken at roughly the saturation intensity of the single ionization process. This allows for a direct comparison between the gases for both the single and double ionization electron spectra. In all cases, the double ionization electron energy distributions are similar and are enhanced at the higher energies compared to the single ionization electrons.

2. Experimental techniques

The acquisition of energy spectra from electrons released in the single ionization process is very straightforward. A simple time-of-flight spectrometer consists of a shielded, field-free region and a detector within a high vacuum chamber. The gas of interest is then backfilled, and an intense, tightly focused laser is used to ionize the atoms. The liberated electrons drift primarily along the polarization direction, where they may be detected after traversing a flight tube. Electrons liberated by a laser pulse have an initial drift velocity at (nearly) zero time, and subsequently drift under no external forces, so their kinetic energy is proportional to $(d/t)^2$, where d is the flight tube length and t is the transit time. Since the single ionization process dominates over the double ionization, the total spectrum is mostly due to single ionization electrons. To extract the greatly outnumbered double ionization electrons from the total spectrum, it is necessary to know which ion was created for each laser shot. By keeping

#30647 - $15.00 US Received February 02, 2001; Revised March 02, 2001

the total count rate low, and recording only those electrons that were detected in coincidence with a doubly charged ion, a double ionization electron spectrum can be compiled.

However, an ordinary ion charge-to-mass spectrometer is not compatible with electron detection. Typically, ions are accelerated towards a detector with a spatially sloped electrostatic potential in the interaction region. The ion arrival times are ordered according to ascending mass-to-charge ratios and are proportional to $(m/q)^{1/2}$, where m is the ion mass and q is its charge. Of course, the static field used to extract the ions would also affect the electrons, destroying their field-free drift. The solution is to pulse the ion extraction field, allowing the electrons to first drift out of the interaction region unaffected before extracting the ions. A single-sided spectrometer, with one detector for both the ions and electrons, was used recently [12]. The spectrometer used in this and a previous study [13] has two distinct halves, one optimized for the collection and detection of ions and the other for electrons.

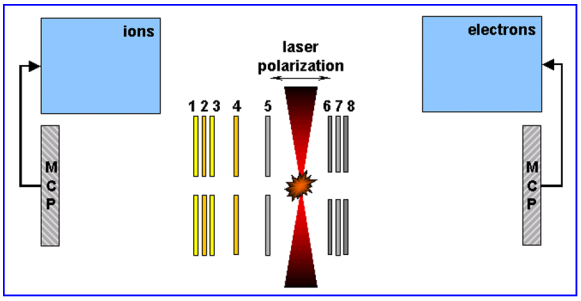

Fig. 1. (55 KB) Animation of the electron-ion spectrometer. The temporal evolution shown is not intended to scale accurately for the ions and electrons. The electron trace is roughly 1 μs long, and the ion trace is roughly 10 μs long.

Figure 1 shows an animation of the electron-ion spectrometer in action. The spectrometer sits within an ultra-high vacuum chamber with a nominal base pressure of 10^{-10} Torr. The entire chamber is backfilled with the gas to be studied while continually pumping with two turbo-molecular pumps. For a given laser intensity and atomic species, the backfill pressure is adjusted for the proper ion detection rate. For the studies described here, 100-fs pulses at 780 nm and at a repetition rate of 1-2 kHz were used. In the figure, the ion micro-channel plate (MCP) detector is on the left, and the electron MCP is on the right. Eight molybdenum field plates are shown numbered. The interaction region is centered between plates 5 and 6, and the entire plate assembly is surrounded by μ-metal shielding. As the laser pulse enters the chamber, plates 5 through 8 are grounded, ensuring a static-field-free region for purely laser-driven electron motion. The liberated electrons (red circles) begin to drift away from the interaction region immediately. The motion of the massive ions (blue circles) is much slower. In the animation, the creation of many ions with a single laser pulse is shown. In reality, the count rate is typically kept low such that multi-ion events are rare. The animation shows only those electrons that pass through the 10º acceptance angle of the plates. Since most electrons are emitted in a small angle peaked along the polarization direction, roughly half (those emitted towards the left) cannot be detected. The electrons emitted towards the right traverse a 20-cm long gold-coated flight tube (not shown) to the electron MCP. A grounded grid at the end of the flight tube minimizes leakage fields from the MCP. At the MCP, the electrons may be detected, contributing to a time-of-flight trace. At a time 150 ns after the laser pulse, plate 5 is biased to a negative voltage (typically –50V to –75V) to extract the ions. At the same time, plate 7 is biased to twice this voltage to block the passage of any secondary electrons. The electrons to the right of the grounded plate 8 are unaffected by the turn-on of plates 5 and 7. With plate 6 grounded and plate 5 biased to a negative voltage, the positively charged ions feel a force towards the left of the figure. The voltages on plates 1 through 4 are chosen to

#30647 - $15.00 US Received February 02, 2001; Revised March 02, 2001

optimize the ion throughput and detection resolution. The ions traverse a 40-cm long biased flight tube towards the ion MCP, where they contribute to a mass-to-charge spectrum. The overall electron collection and detection efficiency is roughly 1%, while the ion collection and detection efficiency is roughly 30%.

3. Coincidence scheme

With this pulsed-plate arrangement, it is possible to detect the electrons and ions generated for any given laser shot. We define a coincidence event as the detection of a single ion and one or more electrons. In this case, it can be determined with some level of certainty that the detected ion and electron were involved in the same ionization process. If the ion detection efficiency were unity, then it would be known with absolute certainty that any electrons must have come from the detected ion. Likewise, if the count rate is kept so low such that two ions are never generated in a single laser shot, then there could never be any ambiguity as to the correlation of the detected ion and electrons. However, for the case of imperfect detectors and reasonable count rates, it is possible that the detected ion and detected electron may come from different ionization events. Coincidence events are therefore classified as "true" when the detected ion and electrons are positively correlated, and accidental or "false" when they are not correlated. For a given set of experimental conditions, a ratio of the true to false counts can be calculated and used in the interpretation of the data [22].

The important factors in determining the true:false ratio are 1) the ion and electron detection efficiencies 2) the relative abundance of the ion of interest, and 3) the total count rate. The first factor is largely determined once a spectrometer is built and optimized, but may vary for different experimental conditions (e.g., if the emittance angle of the electrons changes). Of course, high efficiencies are preferred. The second factor is especially important if the ion of interest makes up a small minority of the total ions, since this increases the likelihood of a false count due to the background ions. The true:false ratio may be improved by minimizing the presence of other ions by keeping the base pressure as low as possible and by using a high purity target gas. However, in the study of doubly charged ions, the "background" is the singly charged ion, and therefore cannot be removed. The ratio of double-to-single ionization events is constant for a particular atomic species at a specific intensity and is typically low. In the experiments discussed here, the double-to-single ionization ratios ranged from 0.029 in Xe to 0.0013 in He. This makes a high true:false ratio difficult to achieve. Finally, the overall count rate represents the simplest way to alter the true:false ratio. In principle, the true:false ratio can be made arbitrarily high by reducing the total count rate, even with poor detection efficiencies and a low relative abundance of the ion of interest. However, in practice, there is a minimum achievable count rate due to background counts. Even with a good vacuum (~10^{-10} Torr), the rate of background ion detection can easily exceed one per five laser shots at high intensities (~1 PW/cm^2). More importantly, even though a reduction in count rate yields a higher true:false ratio, it also greatly reduces the total number of events that are recorded. What one gains in certainty, one inevitably loses in statistical significance. In general, a high-count-rate approach was taken in these experiments.

4. Experimental results

Once the coincidence scheme was tested [13], measurements were made separately with the five readily available noble gases. In order to allow for a direct comparison of all the results, the experimental runs for each gas were taken at roughly the single ionization saturation intensity for each atomic species. Table 1 shows the peak laser intensity used for each gas, as well as the cycle-averaged free-electron quiver energy (U_p, or ponderomotive potential) corresponding to that intensity. The total number of laser shots and the overall ion detection rate are also listed, as is the ratio of double-to-single ionization. Finally, the total number of double ionization coincidence counts and the calculated true:false ratio are given. The true:false values are calculated assuming constant ion and electron collection and detection

#30647 - $15.00 US Received February 02, 2001; Revised March 02, 2001

efficiencies for all ion charges and masses and all electron energies. The exact response of the detectors, as well as changes in the electron angular distributions are not included here.

Table 1. Experimental parameters for the rare gas coincidence survey.

	I_{peak} PW/cm^2	U_p (eV)	N_{shots} ($\times 10^6$)	Ion Det Rate	2+/+ Ratio	N_{coinc} (2+)	T:F (2+)
Helium	0.80	45	200	0.50	0.0013	1058	1.3
Neon	0.60	34	100	0.38	0.0010	700	1.8
Argon	0.25	14	40	0.20	0.0140	1641	3.4
Krypton	0.15	8.5	20	0.20	0.0170	945	3.5
Xenon	0.09	5.1	20	0.20	0.0290	1354	3.5

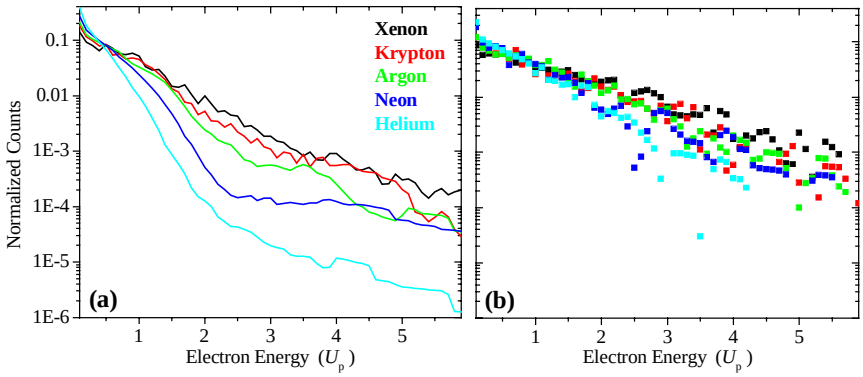

Fig. 2. The electron energy spectra correlated to a) single and b) double ionization.

Figure 2a shows the energy spectra for electrons detected in coincidence with a singly charged ion. Each spectrum is scaled to U_p along the energy (horizontal) axis and the sum of each spectrum is normalized to unity. This allows for direct comparison of the shapes of the distributions. The helium and neon spectra exhibit a sharp drop-off towards $2U_p$ as expected from tunneling. Beyond $2U_p$, elastic backscattering of the electron off the ion core contributes to a long, high-energy plateau. This plateau extends as far as $10U_p$, which is the largest drift energy an electron can gain from the field in the backscattering process. The curves are only shown to $6U_p$, due to the poor statistics on the double ionization curves at higher energies. As a result of the larger scattering cross-section in neon, the neon electron spectrum shows an enhancement at high energies compared to helium. For the higher-Z atoms, the electron spectra become broader, consistent with a transition from the tunneling to multiphoton regime [17]. Figure 2b shows the energy spectra for electrons detected in coincidence with a doubly charged ion. Each spectrum is plotted as in Fig. 2a, and is shown uncorrected for false counts. Correcting the spectra has an effect only at low energies, where there is the greatest abundance of total electrons. In each case, there is an enhancement in relative counts at high energies over the single ionization electrons. Also, in contrast to Fig. 2a, there is a much smaller change in the shapes of the distributions throughout the transition from tunneling to multiphoton ionization. In fact, all the double ionization spectra have similar shapes when scaled to U_p. Of course, in absolute energy units, the electrons from He^{2+} and Ne^{2+} extend much further than those from the double ionization of the higher-Z atoms.

5. Rescattering kinematics

A simple kinematic argument can explain how electrons with high energies might be created in the double ionization process. When an electron is released at rest at the peak of the laser field, it will gain no drift energy. If it is released at a null of the field, it will gain $2U_p$. For

#30647 - $15.00 US
Received February 02, 2001; Revised March 02, 2001

release at all other phases of the field, the electron gains some energy smaller than $2U_p$. This explains the low energy portion of the helium and neon single ionization spectra. If the electron is released with some initial velocity, then it may end up with a larger final energy. In the case of rescattering with the ion core, the electron is instantaneously given a new velocity, and is subsequently accelerated by the laser field. A maximum final energy of $10U_p$ is reached for elastic backscattering at a particular phase of the field [19]. In general, backscattering results in the largest final energies since the electron velocity and driving field have opposite signs. In the single ionization case, this explains the high energy plateau in the spectra. In double ionization, the situation is more complicated but the kinematics are the same. If the first electron has an energy larger than the second electron's binding energy, then it can liberate the second electron through rescattering. Regardless of how the excess energy is shared, the largest final energies will be reached for electrons initially scattered in the backward direction.

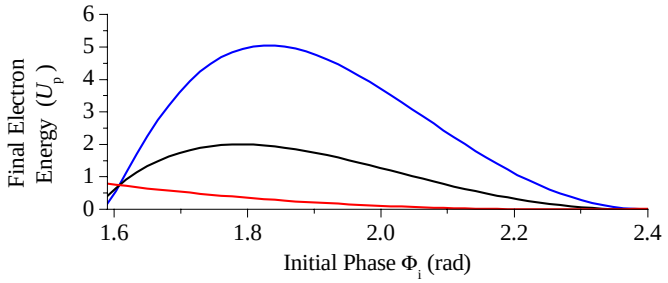

Fig. 3. Final electron energies calculated with a one-dimensional model of helium double ionization at 0.8 PW/cm^2. The cases of zero kinetic energy (black line) after rescattering, initial forward velocity (red line), and initial backward velocity (blue line) are shown.

A simple calculation was performed to demonstrate this argument for the double ionization of helium. First, an elecron is released into a 0.8-PW/cm^2, 780-nm field at an initial phase, Φ_i. If its return energy is sufficient to excite the second electron to its first excited state (40 eV), then any excess energy goes to the first electron in either the forward or backward direction. The second electron is then field ionized with zero initial kinetic energy, and both electrons continue to be driven by the laser field. The final electron energies as a function of the initial phase are shown in Fig. 3. The second electron's energy (black line) is bound by zero and $2U_p$, as is expected for an electron released into the field with zero initial velocity. The forward scattered electron (red line) ends up with even less energy, while the backward scattered electron (blue line) gains as much as $5U_p$. It is a universal feature of rescattering that initally backward velocities are necessary to generate electrons with high energies.

6. Conclusion

We have presented electron energy spectra correlated with the single and double ionization of helium, neon, argon, krypton and helium. In all cases, the electrons released through double ionization are more energetic than those from single ionization. This is compatible with rescattering, where inelastic backscattering can lead to high electron energies. While the single ionization spectra undergo changes consistent with the transition from tunneling to multiphoton ionization, the double ionization spectra remain relatively unchanged. This might imply the presence of a similar rescattering process among all of the rare gases.

Acknowledgments

The experiments were carried out at BNL under contract No. DE-AC02-98CH10886 with the U.S. Dept. of Energy and supported by its Div. of Chemical Sciences (Basic Energy Sciences) and in part under the auspices of the DOE at LLNL under contract No. W-7405-ENG-48.

#30647 - $15.00 US Received February 02, 2001; Revised March 02, 2001